

Grounded Knowledge-Enhanced Medical VLP for Chest X-Ray

Qiao Deng^{1,3[0009-0004-6233-9840]}, Zhongzhen Huang^{5,6[0009-0007-2623-6141]}, Yunqi Wang^{1,3[0000-0002-1584-5132]}, Zhichuan Wang^{1,3[0009-0003-0373-3971]}, Zhao Wang^{4[0000-0003-1860-8391]}, Xiaofan Zhang^{5,6[0000-0003-3999-1449]}, Qi Dou^{4[0000-0002-3416-9950]}, Yeung Yu Hui^{7[0000-0002-4887-7974]}, and Edward S. Hui^{1,2,3[0000-0002-1761-0169]}

¹ Department of Imaging and Interventional Radiology

² Department of Psychiatry

³ CU Lab for AI in Radiology (CLAIR)

⁴ Department of Computer Science and Engineering, The Chinese University of Hong, HKSAR, China

⁵ Shanghai Jiao Tong University, China

⁶ Shanghai AI Laboratory, China

⁷ China Unicorn Global Limited

edward.s.hui@gmail.com

Abstract. Medical vision-language pre-training has emerged as a promising approach for learning domain-general representations of medical image and text. Current algorithms that exploit the global and local alignment between medical image and text could however be marred by the redundant information in medical data. To address this issue, we propose a grounded knowledge-enhanced medical vision-language pre-training (GK-MVLP) framework for chest X-ray. In this framework, medical knowledge is grounded to the appropriate anatomical regions by using a transformer-based grounded knowledge-enhanced module for fine-grained alignment between anatomical region-level visual features and the textural features of medical knowledge. The performance of GK-MVLP is competitive with or exceeds the state of the art on downstream chest X-ray disease classification, disease localization, report generation, and medical visual question-answering tasks. Our results show the advantage of incorporating grounding mechanism to remove biases and improve the alignment between chest X-ray image and radiology report.

Keywords: Medical vision-language pre-training · Grounded knowledge enhancement · Multi-modal representation · Chest X-ray

1 Introduction

Medical data consist of multiple modalities, such as clinical records and medical images. Medical vision-language pre-training (VLP) offers the advantage of learning domain-general representations of medical images and clinical texts.

The model training of medical VLP is however limited by two major issues in the chest X-ray domain. One is the scarcity of labeled data. The other is the challenge in the optimal alignment between the visual information in chest X-ray image and the textural information in radiology report, considering the fact that the former contains fine-grained anatomical and abnormality-specific details, whilst the latter consists of varying levels of granularity. To address these issues, global and local cross-modality alignment and knowledge enhancement strategies have been proposed. ConVIRT [24] globally aligns chest X-ray with radiology report. In addition to global alignment, GloRIA [7], LovT [18] and BioVIL [2] align local image patches with corresponding findings in report. Medical knowledge injection has also been exploited to enhance cross-modality alignment [8,23,20,15].

Considering that contrastive learning-based cross-modality alignment is semantically weak, alignment between image-level abnormality and the corresponding finding in radiology report could be semantically inconsistent. Knowledge enhancement may unfavorably introduce medical knowledge that is not specific to training samples. To this end, we propose a grounded knowledge-enhanced medical vision-language pre-training (GK-MVLP) framework that exploits anatomical region-level grounding of the findings in radiology report to improve the learning of domain-general representations of chest X-ray and radiology report.

The main contributions of this paper are that: (1) we propose a GK-MVLP framework that leverages fine-grained alignment between visual information and medical knowledge to assist representation learning; (2) medical knowledge prompts are constructed to provide instance-level abnormality location information to prevent injecting irrelevant knowledge in the decoding stage; (3) experiments show that GK-MVLP is competitive with or exceeds the performance of the state of the art on downstream disease classification, disease localization, report generation, and medical visual question answering tasks.

2 Method

In this section, we describe the pre-processing of medical knowledge prompts, and the architecture of our proposed GK-MVLP framework, which is based on BLIP [13] and consists of image encoder, report encoder, image-report encoder, report decoder, and grounded knowledge-enhanced (GK) module for aligning medical knowledge prompt with the corresponding anatomical regions. Unless otherwise specified, the following formulation is concerned with a single sample for notional brevity.

2.1 Medical Knowledge Prompts

A medical knowledge prompt Prom is defined as:

$$\text{Prom} = \{\text{entity}_d, \text{position}_d, \text{exist}_d\}_{d=1}^{N_{\text{Abnormality}}}, \quad (1)$$

where entity_d , position_d and exist_d respectively represent the name, position, and existence of the d^{th} most common abnormality, and $N_{\text{Abnormality}}$ is the number of the most common abnormalities on chest X-ray. A list of entities for $N_{\text{Abnormality}} = 14$ most common abnormalities is compiled from all radiology reports (see Appendix Table 1 for the full list). The position of each entity is determined from the subset of 29 different anatomical regions (see Appendix Table 2 for the full list) that are affected by the corresponding abnormality (obtained from the anatomical annotations in the chest ImaGenome dataset [21]). Prom is then constructed by querying the existence of each entity. During pre-training, Prom is converted into a list of sentences, Sentence(Prom), for entities that are present (i.e., $\text{exist}_d = \text{True}$). For instance, $\{\text{pneumonia}, \text{right mid lung zone}, \text{True}\}$ is converted to "Pneumonia is located at right mid lung zone". See Fig. 1a for an overview of the pre-processing of medical knowledge prompts.

2.2 Model Architecture

The overview of the architecture of our proposed GK-MVLP framework is shown in Figs. 1b and 1c.

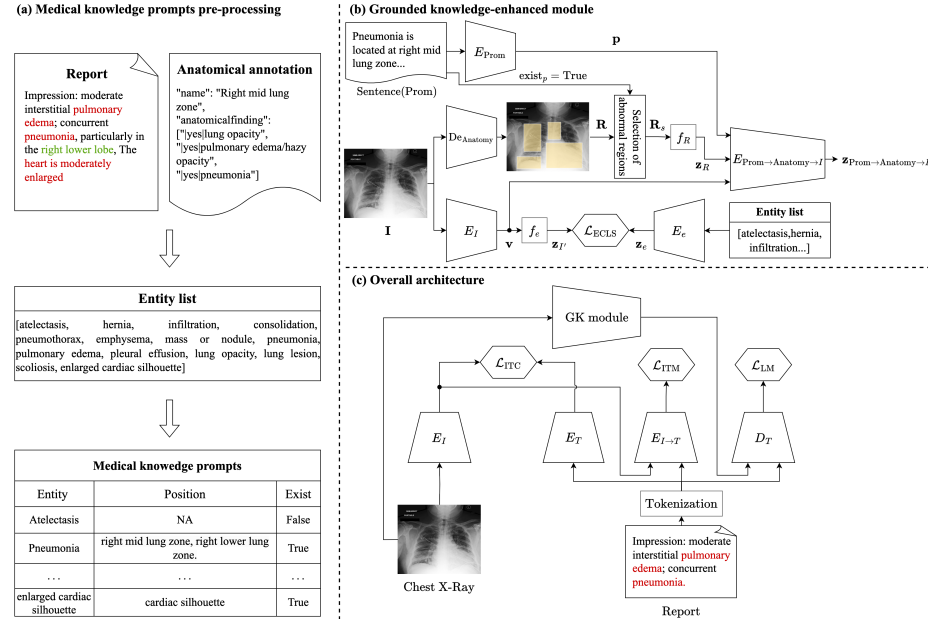


Fig. 1. Illustration of the (a) pre-processing of medical knowledge prompts, and the architecture of the (b) grounded knowledge-enhanced (GK) module and (c) grounded knowledge-enhanced medical vision-language pre-training (GK-MVLP) framework.

Backbone Architecture The backbone architecture of GK-MVLP consists of image encoder E_I , report encoder E_T , image-report encoder $E_{I \rightarrow T}$ and report decoder D_T .

E_I encodes X-ray image \mathbf{I} as a sequence of image embeddings $\mathbf{v} \in \mathbb{R}^{N_I}$, which are subsequently mapped to $\mathbf{z}_I \in \mathbb{R}^{N_P}$ using a projection head f_I :

$$\mathbf{z}_I = f_I(E_I(\mathbf{I})). \quad (2)$$

E_T encodes the tokens of radiology report \mathbf{T} as report embeddings $\mathbf{t} \in \mathbb{R}^{N_T}$, which are subsequently mapped to $\mathbf{z}_T \in \mathbb{R}^{N_P}$ using a projection head f_T :

$$\mathbf{z}_T = f_T(E_T(\mathbf{T})). \quad (3)$$

N_I and N_T denote the dimension of the image and report representation space, respectively. The image and report embeddings are projected onto the same dimension N_P for image-text contrastive (ITC) learning. $E_{I \rightarrow T}$ facilitates the interaction between image and report, and aligns \mathbf{v} to \mathbf{T} and outputs multi-modal feature $\mathbf{z}_{I \rightarrow T}$ for the image-text matching (ITM) task:

$$\mathbf{z}_{I \rightarrow T} = E_{I \rightarrow T}(\mathbf{T}, \mathbf{v}, \mathbf{v}), \quad (4)$$

where $\mathbf{T}, \mathbf{v}, \mathbf{v}$ are respectively the query, key and value. D_T generates radiology report.

Grounded Knowledge-Enhanced Module The GK module consists of entity encoder E_e , knowledge encoder E_{Prom} , pre-trained anatomy detector $\text{De}_{\text{Anatomy}}$, and knowledge-anatomy-image fusion module $E_{\text{Prom} \rightarrow \text{Anatomy} \rightarrow I}$.

E_e encodes the entity list from Prom as $\mathbf{z}_e \in \mathbb{R}^{N_e}$. E_{Prom} encodes the medical knowledge prompt sentences list as prompt embeddings $\mathbf{p} \in \mathbb{R}^{N_{\text{Prom}}}$:

$$\mathbf{p} = E_{\text{Prom}}(\text{Sentence}(\text{Prom})). \quad (5)$$

$\text{De}_{\text{Anatomy}}$ extracts the features of 29 anatomical regions (as defined in the chest ImaGenome) from \mathbf{I} as $\mathbf{R} = [\mathbf{r}_1, \dots, \mathbf{r}_{29}] \in \mathbb{R}^{N_R \times 29}$, where N_R represents the dimension of the anatomical region representation space. The features of anatomical regions that are affected by the abnormalities described in Sentence(Prom) are subsequently selected from \mathbf{R} , $\mathbf{R}_s \in \mathbb{R}^{N_R \times N_{\text{AbRegions}}}$, where $N_{\text{AbRegions}}$ represents the number of anatomical regions that are affected by entities that are present. \mathbf{R}_s is then projected to $\mathbf{z}_R \in \mathbb{R}^{N_{\text{Prom}}}$ using a projection head f_R :

$$\mathbf{z}_R = f_R(\mathbf{R}_s). \quad (6)$$

$E_{\text{Prom} \rightarrow \text{Anatomy} \rightarrow I}$ has two transformer decoder layers, which takes \mathbf{z}_R as a query to iteratively attend to \mathbf{p} for alignment, and outputs local fused features $\mathbf{z}_{\text{Prom} \rightarrow \text{Anatomy}}$. Multi-modal representation is subsequently enhanced by fusing \mathbf{v} with $\mathbf{z}_{\text{Prom} \rightarrow \text{Anatomy}}$ to obtain the global-local fused features $\mathbf{z}_{\text{Prom} \rightarrow \text{Anatomy} \rightarrow I}$:

$$\mathbf{z}_{\text{Prom} \rightarrow \text{Anatomy}} = E_{\text{Prom} \rightarrow \text{Anatomy} \rightarrow I}(\mathbf{z}_R, \mathbf{p}, \mathbf{p}), \quad (7)$$

$$\mathbf{z}_{\text{Prom} \rightarrow \text{Anatomy} \rightarrow I} = E_{\text{Prom} \rightarrow \text{Anatomy} \rightarrow I}(\mathbf{v}, \mathbf{z}_{\text{Prom} \rightarrow \text{Anatomy}}, \mathbf{z}_{\text{Prom} \rightarrow \text{Anatomy}}). \quad (8)$$

$\mathbf{z}_{\text{Prom} \rightarrow \text{Anatomy} \rightarrow I}$ is subsequently injected to D_T to generate a full radiology report.

2.3 Pre-training Objectives

The optimization process during pre-training of GK-MVLP involves four objectives, namely ITC loss \mathcal{L}_{ITC} , ITM loss \mathcal{L}_{ITM} , language modelling (LM) loss \mathcal{L}_{LM} , and entity-based classification loss (ECLS) $\mathcal{L}_{\text{ECLS}}$:

$$\mathcal{L} = \mathcal{L}_{\text{ITC}} + \lambda_1 \mathcal{L}_{\text{ITM}} + \lambda_2 \mathcal{L}_{\text{LM}} + \lambda_3 \mathcal{L}_{\text{ECLS}}. \quad (9)$$

We adopted \mathcal{L}_{ITC} , \mathcal{L}_{ITM} , \mathcal{L}_{LM} from [13,14]. \mathcal{L}_{ITC} aligns \mathbf{z}_I and \mathbf{z}_T . \mathcal{L}_{ITM} permits fine-grain alignment between image and report by distinguishing whether an image-report pair is positive or negative given $\mathbf{z}_{I \rightarrow T}$. \mathcal{L}_{LM} supervises the report generation for D_T given $\mathbf{z}_{\text{Prom} \rightarrow \text{Anatomy} \rightarrow I}$ through minimization of the cross-entropy loss.

$\mathcal{L}_{\text{ECLS}}$ associates \mathbf{I} with the corresponding entities, and aims to align \mathbf{v} with \mathbf{z}_e by calculating their similarity, followed by a binary cross entropy loss \mathcal{L}_{BCE} :

$$\mathcal{L}_{\text{ECLS}} = \mathcal{L}_{\text{BCE}}(\mathbf{z}_{I'} \cdot \mathbf{z}_e, \text{Token}_{\text{exist}}), \quad (10)$$

where $\mathbf{z}_{I'}$ is mapped from \mathbf{v} using projection head f_e , and $\text{Token}_{\text{exist}}$ is 1 when exist=True and 0 otherwise.

3 Experiment

3.1 Datasets

Pre-training The findings and impression sections are extracted from the radiology reports in the MIMIC-CXR dataset [10]. Medical knowledge prompts are generated from the attributes of anatomical regions in the Chest ImaGenome dataset [21].

Fine-tuning Pre-trained GK-MVLP is evaluated on 4 downstream tasks, namely disease classification (fine-tuned on the RSNA Pneumonia [11], NIH ChestX-ray [19], CheXpert [9] datasets), disease localization (RSNA Pneumonia), report generation (IU X-Ray [4]), and medical visual question answering, Med-VQA, (VQA-RAD [12]). Note that different subsets of the RSNA Pneumonia dataset are used for the disease classification and localization tasks. See Table 1 for task-specific data splitting strategy.

3.2 Implementation Details

The vision transformer (ViT-B/16 [5]) is adopted as the image encoder. SciBERT [1] is adopted as report encoder, knowledge encoder and entity encoder. A 12-layer transformer encoder is adopted as the image-report encoder with hidden state dimensions set to 768. Another 12-layer transformer decoder is adopted as the report decoder. The AdamW optimizer with weight decay of 0.05, learning rate of 3e-4 with a decay rate of 0.9, and a warm-up period of 3000 steps are applied. The model is pre-trained on 8 NVIDIA A6000 GPUs, with a batch size of 32, for 20 epochs. $\lambda_1, \lambda_2, \lambda_3$ are set to 1.

Table 1. Data splitting strategy for pre-training and fine-tuning.

| | Dataset | Training | Validation | Testing |
|------------------------|-----------------|----------|------------|---------|
| Pre-training | | | | |
| | MIMIC-CXR | 166504 | - | - |
| | Chest ImaGenome | 166504 | - | - |
| Fine-tuning | | | | |
| Disease classification | RSNA Pneumonia | 25184 | 1500 | 3000 |
| | NIH ChestX-ray | 78468 | 11219 | 22433 |
| | CheXpert | 218414 | 5000 | 234 |
| Disease localization | RSNA Pneumonia | 16010 | 5337 | 5227 |
| Report generation | IU X-Ray | 2069 | 296 | 590 |
| | Med-VQA | 3064 | - | 451 |
| | VQA-RAD | | | |

3.3 Comparison With State-Of-The-Arts

Our proposed GK-MVLP is pre-trained on 160,000 image-report pairs from the Chest ImaGenome dataset.

Label-Efficient Disease Classification Pre-trained GK-MVLP are fine-tuned on 1%, 10%, and 100% of 3 widely-used chest X-ray datasets. Comparisons with GLoRIA (pre-trained on 190,000 images from CheXpert), and ConVIRT, BioViL, MedKLIP [20], and M-FLAG [16] (pre-trained on 370,000 images from MIMIC-CXR) are shown in Table 2. Apart from the few-shot experiments on the NIH ChestX-ray and CheXpert datasets, our pre-trained GK-MVLP outperforms SOTAs by up to 9.1.

Label-Efficient Disease Localization Pre-trained GK-MVLP are fine-tuned on 1%, 10%, and 100% of the RSNA Pneumonia dataset. Comparisons with LoVT, SimCLR [3], BYOL [6], and PixelPro [22] are shown in Table 3. Compared to GK-MVLP with random initialization, pre-trained GK-MVLP consistently perform better across all experiments. Apart from the few-shot experiments, GK-MVLP outperforms SOTAs with performance gain up to 2.6%.

Report Generation and Med-VQA Pre-trained GK-MVLP is respectively fine-tuned on IU X-Ray and VQA-RAD datasets for the report generation and Med-VQA tasks. Comparisons with MedViLL [17] and MOTOR are shown in Table 4. Of note is that GK-MVLP and MOTOR employ the same backbone model, BLIP, for pre-training. Our model outperforms MOTOR by 0.012 in BLEU₄ score for the report generation task and 1.8% in the overall accuracy for the Med-VQA task.

Ablations Experiments are conducted to investigate the effect of different components of our proposed GK modules on the model performance of vanilla model

Table 2. Comparison of area-under-the-curve scores for disease classification task with different training dataset sizes.

| Method | RSNA Pneumonia | | | NIH ChestX-ray | | |
|-------------|-----------------|-----------------|-----------------|----------------|-----------------|-----------------|
| | 1% | 10% | 100% | 1% | 10% | 100% |
| GLoRIA | 86.1 | 88.0 | 88.6 | - | - | - |
| ConVIRT | 88.8 | 91.5 | 92.7 | - | - | - |
| BioViL | 88.1 | 88.4 | 89.1 | - | - | - |
| MedKLIP | 87.3 | 88.0 | 89.3 | 77.2 | 78.9 | 83.2 |
| M-FLAG [16] | - | - | - | 62.2 | 71.6 | 78.7 |
| Ours | 90.0±0.2 | 91.7±0.2 | 92.7±0.1 | 74.9±0.3 | 80.7±0.3 | 84.5±0.1 |

| | CheXpert | | |
|---------|-------------|-----------------|-----------------|
| | 1% | 10% | 100% |
| GLoRIA | 86.6 | 87.8 | 88.1 |
| ConVIRT | 87.0 | 88.1 | 88.1 |
| BioViL | - | - | - |
| MedKLIP | - | - | - |
| M-FLAG | - | - | - |
| Ours | 86.7±0.2 | 88.8±0.1 | 89.2±0.2 |

Table 3. Comparisons of mean average precision (%) for disease localization task with different training dataset sizes.

| Method | RSNA Pneumonia | | |
|------------------------------|----------------|-----------------|-----------------|
| | 1% | 10% | 100% |
| LoVT | 8.5±0.8 | 13.2±0.6 | 18.1±3.2 |
| SimCLR | 7.1±0.7 | 12.2±0.8 | 18.8±1.0 |
| BYOL | 5.6±0.8 | 11.0±0.2 | 17.3±1.1 |
| PixelPro | 4.8±0.3 | 11.0±1.5 | 17.4±1.7 |
| Ours (random initialization) | 3.3±0.3 | 8.3±0.6 | 15.8±1.2 |
| Ours | 6.9±0.5 | 13.6±0.2 | 19.9±0.2 |

Table 4. Comparisons of natural language generation metrics for report generation task and accuracy (%) for Med-VQA task.

| Method | Report Generation | | | Med-VQA | | |
|---------|-------------------|--------------|--------------------|--------------|-------------|-------------|
| | BLEU ₄ | METEOR | ROUGE _L | Open | Closed | Overall |
| | | | | Accuracy (%) | | |
| MedViLL | 0.049 | - | - | 59.5 | 77.7 | - |
| MOTOR | 0.156 | 0.193 | 0.314 | 64.8 | 74.6 | 70.7 |
| Ours | 0.168 | 0.199 | 0.329 | 64.8 | 77.6 | 72.5 |

(i.e., BLIP) for the report generation task (see Table 5). Compared to BLIP, incorporating medical knowledge prompts alone (second and third rows) depre-

ciates model performance, suggesting that the correlation between chest X-ray image and prompt is poor. Adding the anatomical region-specific visual information alone (forth and fifth rows) also depreciates model performance, suggesting that anatomical annotations alone do not improve cross-modality representation learning. Compared to BLIP and experiments that incorporate both prompt and anatomical regions to the baseline model (sixth and seventh rows), there is appreciable performance gain with the addition of the knowledge-anatomy-image fusion module (second last row) indicating the clear benefit of grounding mechanism. Finally, selection of abnormal anatomical regions for grounding medical knowledge, i.e. our proposed GK-MVLP, yielded the best model performance. Taken together, cross-modality representation learning can be improved by our proposed GK-MVLP framework which offers additional information from grounding medical knowledge with the corresponding abnormal anatomical regions.

Table 5. Ablation study of our proposed GK-MVLP framework on the report generation task.

| Method | BLEU ₄ | METEOR | ROUGE _L |
|---|-------------------|--------------|--------------------|
| 1 Villa BLIP | 0.159 | 0.196 | 0.321 |
| 2 + Prom | 0.157 | 0.191 | 0.314 |
| 3 + Prom + \mathcal{L}_{ECLS} | 0.158 | 0.196 | 0.320 |
| 4 + De _{Anatomy} | 0.163 | 0.190 | 0.319 |
| 5 + De _{Anatomy} + \mathcal{L}_{ECLS} | 0.160 | 0.192 | 0.317 |
| 6 + Prom + De _{Anatomy} | 0.162 | 0.194 | 0.321 |
| 7 + Prom + De _{Anatomy} + \mathcal{L}_{ECLS} | 0.165 | 0.194 | 0.317 |
| 8 GK-MVLP (w/o selection of abnormal regions) | 0.166 | 0.197 | 0.319 |
| 9 GK-MVLP | 0.168 | 0.199 | 0.329 |

4 Conclusion

We present a grounded knowledge-enhanced medical vision-language pre-training framework to improve the learning of domain-general representations of chest X-ray and radiology report. Our result show that grounding medical knowledge with the appropriate anatomical regions permits performance gain in various chest X-ray tasks.

References

1. Beltagy, I., Lo, K., Cohan, A.: Scibert: A pretrained language model for scientific text. arXiv preprint arXiv:1903.10676 (2019)

2. Boecking, B., Usuyama, N., Bannur, S., Castro, D.C., Schwaighofer, A., Hyland, S., Wetscherek, M., Naumann, T., Nori, A., Alvarez-Valle, J., et al.: Making the most of text semantics to improve biomedical vision–language processing. In: European conference on computer vision. pp. 1–21. Springer (2022)
3. Chen, T., Kornblith, S., Norouzi, M., Hinton, G.: A simple framework for contrastive learning of visual representations. In: International conference on machine learning. pp. 1597–1607. PMLR (2020)
4. Demner-Fushman, D., Kohli, M.D., Rosenman, M.B., Shooshan, S.E., Rodriguez, L., Antani, S., Thoma, G.R., McDonald, C.J.: Preparing a collection of radiology examinations for distribution and retrieval. Journal of the American Medical Informatics Association **23**(2), 304–310 (2016)
5. Dosovitskiy, A., Beyer, L., Kolesnikov, A., Weissenborn, D., Zhai, X., Unterthiner, T., Dehghani, M., Minderer, M., Heigold, G., Gelly, S., et al.: An image is worth 16x16 words: Transformers for image recognition at scale. arXiv preprint arXiv:2010.11929 (2020)
6. Grill, J.B., Strub, F., Altché, F., Tallec, C., Richemond, P., Buchatskaya, E., Doersch, C., Avila Pires, B., Guo, Z., Gheshlaghi Azar, M., et al.: Bootstrap your own latent-a new approach to self-supervised learning. Advances in neural information processing systems **33**, 21271–21284 (2020)
7. Huang, S.C., Shen, L., Lungren, M.P., Yeung, S.: Gloria: A multimodal global-local representation learning framework for label-efficient medical image recognition. In: Proceedings of the IEEE/CVF International Conference on Computer Vision. pp. 3942–3951 (2021)
8. Huang, Z., Zhang, X., Zhang, S.: Kiut: Knowledge-injected u-transformer for radiology report generation. In: Proceedings of the IEEE/CVF Conference on Computer Vision and Pattern Recognition. pp. 19809–19818 (2023)
9. Irvin, J., Rajpurkar, P., Ko, M., Yu, Y., Ciurea-Ilcus, S., Chute, C., Marklund, H., Haghgoo, B., Ball, R., Shpanskaya, K., et al.: Chexpert: A large chest radiograph dataset with uncertainty labels and expert comparison. In: Proceedings of the AAAI conference on artificial intelligence. vol. 33, pp. 590–597 (2019)
10. Johnson, A.E., Pollard, T.J., Greenbaum, N.R., Lungren, M.P., Deng, C.y., Peng, Y., Lu, Z., Mark, R.G., Berkowitz, S.J., Horng, S.: Mimic-cxr-jpg, a large publicly available database of labeled chest radiographs. arXiv preprint arXiv:1901.07042 (2019)
11. Kaggle, R.: Pneumonia detection challenge. URL: <https://www.kaggle.com/c/rsna-pneumonia-detection-challenge> (2020)
12. Lau, J.J., Gayen, S., Ben Abacha, A., Demner-Fushman, D.: A dataset of clinically generated visual questions and answers about radiology images. Scientific data **5**(1), 1–10 (2018)
13. Li, J., Li, D., Xiong, C., Hoi, S.: Blip: Bootstrapping language-image pre-training for unified vision-language understanding and generation. In: International Conference on Machine Learning. pp. 12888–12900. PMLR (2022)
14. Li, J., Selvaraju, R., Gotmare, A., Joty, S., Xiong, C., Hoi, S.C.H.: Align before fuse: Vision and language representation learning with momentum distillation. Advances in neural information processing systems **34**, 9694–9705 (2021)
15. Lin, B., Chen, Z., Li, M., Lin, H., Xu, H., Zhu, Y., Liu, J., Cai, W., Yang, L., Zhao, S., et al.: Towards medical artificial general intelligence via knowledge-enhanced multimodal pretraining. arXiv preprint arXiv:2304.14204 (2023)
16. Liu, C., Cheng, S., Chen, C., Qiao, M., Zhang, W., Shah, A., Bai, W., Arcucci, R.: M-flag: Medical vision-language pre-training with frozen language models and

latent space geometry optimization. In: International Conference on Medical Image Computing and Computer-Assisted Intervention. pp. 637–647. Springer (2023)

- 17. Moon, J.H., Lee, H., Shin, W., Kim, Y.H., Choi, E.: Multi-modal understanding and generation for medical images and text via vision-language pre-training. *IEEE Journal of Biomedical and Health Informatics* **26**(12), 6070–6080 (2022)
- 18. Müller, P., Kaassis, G., Zou, C., Rueckert, D.: Joint learning of localized representations from medical images and reports. In: European Conference on Computer Vision. pp. 685–701. Springer (2022)
- 19. Wang, X., Peng, Y., Lu, L., Lu, Z., Bagheri, M., Summers, R.M.: Chestx-ray8: Hospital-scale chest x-ray database and benchmarks on weakly-supervised classification and localization of common thorax diseases. In: Proceedings of the IEEE conference on computer vision and pattern recognition. pp. 2097–2106 (2017)
- 20. Wu, C., Zhang, X., Zhang, Y., Wang, Y., Xie, W.: Medklip: Medical knowledge enhanced language-image pre-training. medRxiv pp. 2023–01 (2023)
- 21. Wu, J., Agu, N., Lourentzou, I., Sharma, A., Paguio, J., Yao, J.S., Dee, E.C., Mitchell, W., Kashyap, S., Giovannini, A., et al.: Chest imangenome dataset. *PhysioNet* (2021)
- 22. Xie, Z., Lin, Y., Zhang, Z., Cao, Y., Lin, S., Hu, H.: Propagate yourself: Exploring pixel-level consistency for unsupervised visual representation learning. In: Proceedings of the IEEE/CVF Conference on Computer Vision and Pattern Recognition. pp. 16684–16693 (2021)
- 23. Zhang, X., Wu, C., Zhang, Y., Xie, W., Wang, Y.: Knowledge-enhanced visual-language pre-training on chest radiology images. *Nature Communications* **14**(1), 4542 (2023)
- 24. Zhang, Y., Jiang, H., Miura, Y., Manning, C.D., Langlotz, C.P.: Contrastive learning of medical visual representations from paired images and text. In: Machine Learning for Healthcare Conference. pp. 2–25. PMLR (2022)